ELSEVIER

Chemical Engineering Journal 70 (1998) 47–54

Chemical Engineering Journal

Catalytic pyrolysis of methylcyclohexane: kinetics and modeling

K.K. Pant, D. Kunzru *

Department of Chemical Engineering, Indian Institute of Technology, Kanpur-208016, India

Received 12 August 1997; revised 23 December 1997; accepted 5 January 1998

Abstract

Steam pyrolysis of methylcyclohexane has been studied over potassium carbonate impregnated calcium aluminate catalyst in a fixed bed reactor at atmospheric pressure in the temperature range of 973–1073 K. Compared to noncatalytic pyrolysis, the conversion was significantly higher but the hydrocarbon product selectivities were not affected in the presence of the catalyst. Incorporation of K_2CO_3 in the catalyst significantly reduced the coke deposited on the catalyst. The overall catalytic pyrolysis reaction could be represented by a first-order reaction with a preexponential factor of 1.1×10^3 $m^3/(kg\ s)$ and an activation energy of 106.9 kJ/mol. The experimental product yields could be satisfactorily modeled by use of a molecular reaction scheme, consisting of a first-order primary reaction and twenty four secondary reactions among the primary products.

Keywords: Catalytic pyrolysis; Calcium aluminate; Kinetics; Methylcyclohexane; Pyrolysis modeling

1. Introduction

Noncatalytic steam pyrolysis of petroleum fractions is the usual process for producing light olefins, such as ethylene, propylene and butenes. The possibility of improving the pyrolysis process by the introduction of calcium aluminate catalyst has been studied by several investigators [1–6]. The main aim of catalyst development is to either lower the reaction temperature for the same throughput, reduce the coke formation or increase the yield of desired products. The limited data on catalytic pyrolysis has been summarized by Basu and Kunzru [5]. Except for Nowak et al. [4], who used calcium aluminate containing 30% CaO, the other studies have found $12CaO–7Al_2O_3$ to be the most active crystalline phase. A limitation of the calcium aluminate catalyst is the coke deposition on the catalyst. The coke deposition on the catalyst was significantly decreased when calcium aluminate was impregnated with K_2CO_3 [6] or proprietary promoters [4] to enhance the coke-steam reaction. Most of the studies on catalytic pyrolysis have focused on petroleum fractions [1,2,4–6] or *n*-paraffins such as *n*-hexane [3,7] and *n*-heptane [8,9]. No published data is available on the catalytic pyrolysis of naphthenes, which are present in significant amount in naphtha. Since methylcyclohexane is the predominant alkylcyclohexane in naphtha, it was chosen as the representative compound of this homologous series.

The objective of this study was to investigate the effect of process variables on the conversion and product yields during the pyrolysis of methylcyclohexane on potassium carbonate impregnated calcium aluminate catalyst and the possibility of reducing the operating temperature by use of a catalyst. Another objective was to determine the kinetics and develop a model for this reaction. The kinetics and modeling of noncatalytic pyrolysis of methylcyclohexane has been published earlier [10].

2. Experimental

2.1. Catalyst preparation and characterization

It was found that the method of preparation of CaO had a significant effect on the structural strength of the catalyst and for this study, CaO was prepared by the decomposition of $Ca(OH)_2$ at 1023 K for 3 h. To prepare the $12CaO–7Al_2O_3$ catalyst, required amounts of CaO and Al_2O_3 were mixed in the presence of a binder (1% aqueous solution of polyvinyl alcohol), moulded into cylindrical pellets, aged at 353 K for 24 h and then sintered at 1623 K for 18 h. K_2CO_3 was impregnated on the calcium aluminate by incipient wetness technique, followed by heat-treatment at 1023 K for 6 h. The initial K_2CO_3 loading on the catalyst was 10 wt.% (corresponding to a potassium content of 5.7 wt.%); however, due to the potassium loss during heat-treatment, the potassium

* Corresponding author.

1385-8947/98/$19.00
PII S1385-8947(98)00073-4

Table 1
Effect of potassium impregnation on calcium aluminate catalyst on conversion, product yields and coke deposited during methylcyclohexane pyrolysis

	Noncatalytic pyrolysis	Calcium aluminate	4.8 wt.% potassium impregnated calcium aluminate
Conversion %	52.0	71.5	70.5
Product yields (wt.% MCH)			
Methane	5.8	8.2	8.0
Ethylene	12.2	19.2	18.7
Propylene	9.4	10.6	10.4
1,3-Butadiene	8.2	10.8	10.9
Isoprene	1.7	2.6	2.7
Cyclohexene	1.4	1.6	1.6
Benzene	4.0	5.3	5.0
Toluene	0.5	3.5	3.5
Carbon monoxide	0.0	tr	0.3
Carbon dioxide	tr	0.5	1.7
Other products	6.5	8.5	7.9
Coke on catalyst after a run time of 3 h (wt.%)	–	5.8	1.4

Catalyst zone temperature = 1023 K; $\delta = 2.5$ (kg steam)/(kg MCH); $W/m_{A_0} = 300$ (kg cat s)/(kg MCH).
tr: trace.

content of the fresh catalyst used in the pyrolysis runs was 4.8 wt.%. For the pyrolysis runs, the catalyst was crushed and sieved, and the 2.5 ± 0.5 mm size fraction retained for use. Runs made with a smaller catalyst size fraction of 1.0–1.4 mm confirmed that there was no effect of catalyst size on the conversion and product yields.

The prepared catalysts were characterized using X-ray diffraction, surface area and atomic absorption spectroscopy. The details regarding catalyst characterization have been presented earlier [8]. The diffraction pattern of the K_2CO_3 impregnated calcium aluminate confirmed that the major crystalline phase was $12CaO–7Al_2O_3$ whereas $3CaO–Al_2O_3$ was present in minor amounts. A comparison of the diffraction pattern of the promoted and unpromoted calcium aluminate showed that no new crystalline phase was formed due to K_2CO_3 impregnation. The total surface area of the K_2CO_3 impregnated calcium aluminate catalyst was 0.7 ± 0.1 m^2/g.

2.2. Apparatus and procedure

The pyrolysis runs were conducted in a tubular reactor and the experimental apparatus was the same as that used for an earlier study on catalytic pyrolysis of *n*-heptane [8]. The stainless steel reactor (19 mm i.d., 25 mm o.d.) was heated in a three-zone furnace. The heated length was 600 mm. Methylcyclohexane (MCH) and water were pumped from separate burettes using metering pumps. During the course of a run, the total condensed liquid, together with the volume and composition of the gaseous effluent was measured at regular intervals. After the completion of the run, the reactor was flushed with steam for 1 h, and then either the reactor was decoked with air or the coked catalyst was removed from the reactor for determination of the coke content.

The noncondensable, which mainly consisted of $C_1–C_4$ hydrocarbons, CO and CO_2 were analyzed by gas chromatography using three columns [8]. The liquid products were analyzed on a capillary column (Petrocol DH column, i.d.: 0.25 mm, length: 100 m).

3. Results and discussion

Catalytic pyrolysis of methylcyclohexane was conducted in the presence of steam at atmospheric pressure for various temperatures, space times and steam dilution ratios. The experiments covered the following range of variables: temperature, 973 to 1073 K, methylcyclohexane flow rate, 0.3 to 2.9 g/min, steam flow rate, 0.6 to 6.0 g/min, mass of catalyst/mass flow rate of MCH, 150 to 390 (kg cat s)/kg. The inlet steam to MCH ratio was varied from 2.0 to 3.0 kg/kg. To passivate the reactor walls, 200 ppm carbon disulfide was added to the hydrocarbon feed.

To check the effect of impregnation, some runs at identical conditions were made with potassium-free as well as K_2CO_3 impregnated calcium aluminate. Compared to noncatalytic pyrolysis, the conversion as well as the product yields were significantly increased in both cases (Table 1). As can be seen from Table 1, compared to calcium aluminate, addition of K_2CO_3 to the calcium aluminate only marginally affected the overall conversion and hydrocarbon product yields. On the other hand, with K_2CO_3-impregnated catalyst, the coke deposited on the catalyst was significantly lower and yield of carbon oxides appreciably higher. A similar effect of K_2CO_3 impregnation has also been reported during catalytic pyrolysis of naphtha [6] and *n*-heptane [8]. Due to the significantly lower coke deposition on the K_2CO_3 impregnated catalyst, subsequent runs were made using this catalyst only. It should be mentioned that although there was an appreciable potassium loss from the catalyst during reaction (the potassium loss from the catalyst during a 3 h run at 1023 K was approximately 40%), this did not have any affect on the

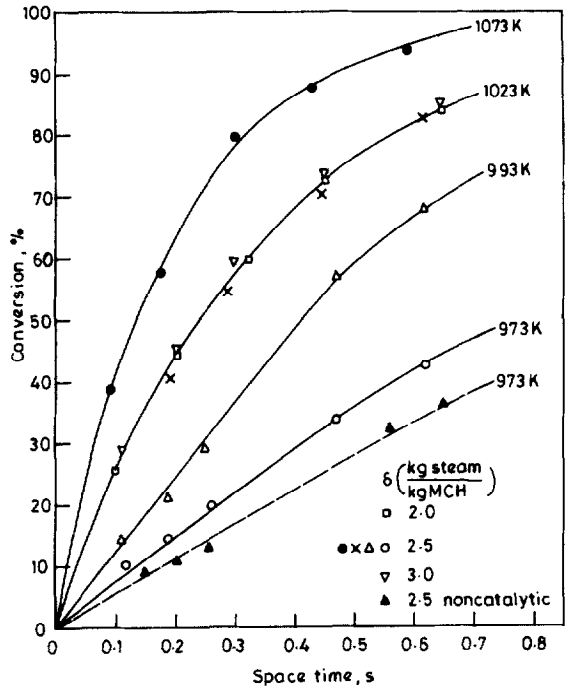

Fig. 1. Variation of methylcyclohexane conversion with space time.

catalyst activity or selectivity during a run which was usually of 3 h duration.

3.1. Kinetic analysis

The variation of MCH conversion with space time (τ) at various temperatures is shown in Fig. 1. For the sake of comparison, the conversion obtained for noncatalytic pyrolysis of MCH at 973 K [10] is also shown in this figure. Although there were significant axial temperature gradients at the entrance and exit, the temperature in the central portion of the reactor, which extended from approximately 20 to 40 cm from the reactor inlet, was uniform. The catalyst was positioned in this isothermal zone and the temperatures indicated in Fig. 1 refer to the catalytic zone temperature. The space time for each run was evaluated using the pseudoisothermal approach based on the equivalent reactor volume concept [11]. However, for the kinetic analysis the actual temperature profile for each run was used.

As can be seen from Fig. 1, conversion increased significantly in the presence of the catalyst. For instance, at 973 K the conversion for noncatalytic pyrolysis at a space time 0.25 s was 12.5% whereas at similar conditions, the conversion for catalytic pyrolysis was 19.5%. A similar effect was observed at other temperatures also. As is also shown in this figure, increasing δ from 2.0 to 3.0 kg steam/kg MCH had no noticeable effect on the conversion.

During a catalytic run, both thermal and catalytic pyrolysis occur simultaneously, and in order to determine the kinetics of catalytic pyrolysis, the kinetics of noncatalytic pyrolysis is required. Pant and Kunzru [10] determined the kinetics of noncatalytic pyrolysis of MCH by using nonlinear optimization and reported the overall reaction order, preexponential factor and activation energy to be 1, 1.7×10^{11} s^{-1} and 209.0 kJ/mol, respectively.

During catalytic pyrolysis, there were three zones in the reactor. In the first zone, which extended from the reactor inlet to a length L_1, only thermal pyrolysis took place. In the second catalytic zone, from length L_1 to L_2, both catalytic and thermal reactions occurred simultaneously, whereas in the third zone, from L_2 to the reactor exit L, only noncatalytic pyrolysis occurred.

Since the conversion of MCH was independent of δ (Fig. 1), the overall reaction order for the catalytic pyrolysis of MCH was taken to be one. Making a differential mass balance in the catalytic zone and integrating, we obtain [8]

$$(1+\varepsilon)\ln\left[\frac{1-X_{A1}}{1-X_{A2}}\right]-\varepsilon(X_{A2}-X_{A1}) = \frac{A_c}{Q_o}\left[k_t\varepsilon_B+k_tV_g\rho_p(1-\varepsilon_B)+k_c\rho_p(1-\varepsilon_B)\right](L_2-L_1) \quad (1)$$

In Eq. (1), the noncatalytic pyrolysis reactions in the void region between the catalyst particles as well as in the intraparticle space have been accounted for. ρ_p and ε_B were experimentally measured to be 1700 kg/m^3 and 0.35, respectively. Due to the high steam dilution, the volume change due to reaction was not appreciable (ε varied from 0.12 at a conversion of 10.0% to 0.16 at a conversion of 93.5%). The inlet and outlet conversions of the catalytic zone were estimated by numerically integrating the differential mass balance equations in the first and third thermal zones, using the known kinetics of noncatalytic pyrolysis [10], the measured axial temperature profile and the exit conversion. The rate constants for catalytic pyrolysis, k_c, at different temperatures were then determined from the slopes of the plot of the left-hand side of Eq. (1) vs. $A_c(L_2-L_1)/Q_o$ (Fig. 2) and are given in Table 2. For the sake of comparison, the values of k_t have also been shown. The activation energy and preexponential factor, as obtained from an Arrhenius plot, were 106.9 kJ/mol and 1.1×10^3 m^3/(kg cat s), respectively. These values are in good agreement with the activation energies of 109.4 kJ/mol and 103.8 kJ/mol reported for the catalytic pyrolysis of *n*-hexane [7] and *n*-heptane [8], respectively.

Thus, the catalyst significantly increased the rate of reaction, reducing the temperature required to achieve a given percentage conversion by approximately 35 K.

3.2. Product distribution

The effect of process variables on the product yields (wt.% feed) and selectivities (moles product/100 moles MCH decomposed) was investigated. As in the case of noncatalytic pyrolysis of MCH [10], the main products were methane, ethylene, propylene, 1,3-butadiene, cyclohexene, benzene, toluene and isoprene, whereas methylcyclohexenes, and pentadienes were formed as minor products. Small amounts of carbon oxides were also formed in all the catalytic runs.

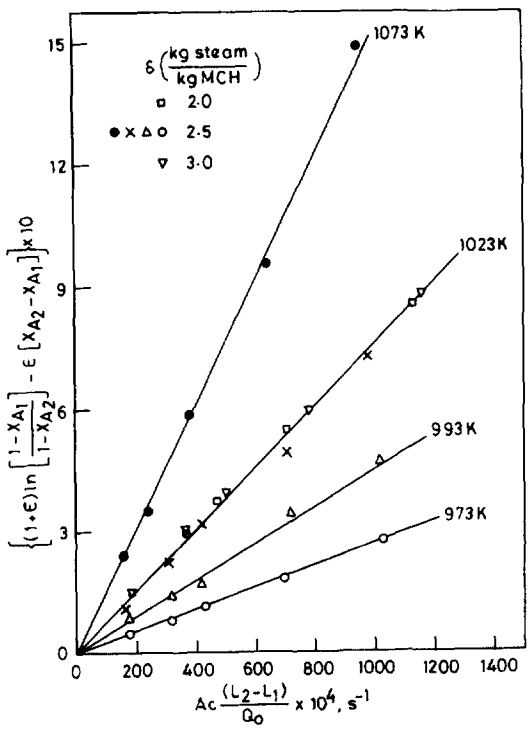

Fig. 2. Determination of the first-order rate constant at different temperatures for catalytic pyrolysis.

Table 2
Rate constants for the pyrolysis of methylcyclohexane

Temperature (K)	k_1 s^{-1}	$k_c \times 10^3$ $m^3/(kg\ s)$	$k_c \rho_b$ s^{-1}
973	1.0	1.8	3.1
993	1.7	2.7	4.6
1023	3.5	4.1	7.0
1073	11.2	5.7	9.7

To study the effect of temperature on product yields, catalytic runs were made at different temperatures for the same δ, W/m_{A0} and τ. Since the calculated τ depends on the axial temperature profile, τ was not exactly the same for the different runs but varied between 0.43 to 0.47 s. The variation in the yields of CH_4, C_2H_4 and C_3H_6 with temperature is shown in Fig. 3. The yields of CH_4 and C_2H_4 increased with temperature and were significantly higher in the presence of the catalyst. In contrast to noncatalytic pyrolysis, the yield of C_3H_6 showed a maximum with increasing temperature.

The variation of product selectivities with conversion for the main primary products at different temperatures is shown in Fig. 4, whereas the detailed product selectivities for some selected runs are shown in Table 3. For a fixed conversion, there was no noticeable effect of temperature on selectivities. At all conditions, ethylene was the main product and its yield varied from 2.0 wt.% feed at low conversion to 28.7 wt.% feed at the highest conversion (93.5%) studied. Depending on the primary and secondary reactions, the selectivities of the various products either increased (methane, ethylene and benzene), decreased (isoprene, cyclohexene and toluene) or

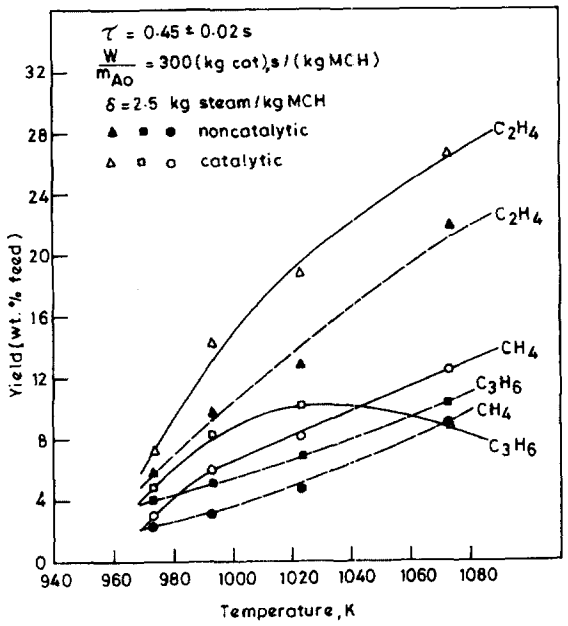

Fig. 3. Effect of temperature on methane, ethylene and propylene yields.

showed a maximum (propene and 1,3-butadiene) with increasing conversion. In the range investigated, there was no noticeable effect of steam dilution on the product yields (refer run nos. MC5, MC6, MC7, Table 3). The probable primary and secondary reactions during the pyrolysis of MCH have been discussed elsewhere [10,12].

In contrast to the results of noncatalytic pyrolysis of MCH [10], measurable amounts of CO and CO_2 were obtained in each run (refer Table 3). The yields of carbon oxides increased with conversion and were higher at higher δ. On the other hand, the coke deposited on the catalyst increased with conversion and was lower at higher steam dilution.

A comparison of the product distribution obtained during catalytic and noncatalytic pyrolysis [10] showed that except for carbon oxides, the product selectivities at a fixed conversion were approximately equal. During pyrolysis, several initiation, propagation and termination reactions occur simultaneously and the product distribution mainly depends on the propagation and termination steps. This suggests that the catalyst does not affect the pyrolysis mechanism and only increases the rate of the initiation steps. Similar results have been reported for the catalytic pyrolysis of *n*-heptane [8].

4. Model development

A molecular model, consisting of a first-order primary reaction and 24 secondary reactions, developed earlier for noncatalytic pyrolysis of methylcyclohexane [10] was modified to calculate the product yields during catalytic pyrolysis of MCH. The development of the model was based on the experimental observation that the variation of product selectivities with conversion was not affected by the catalyst. Thus, for catalytic pyrolysis only the rate constant and the activation energy of the first-order primary step were changed, whereas

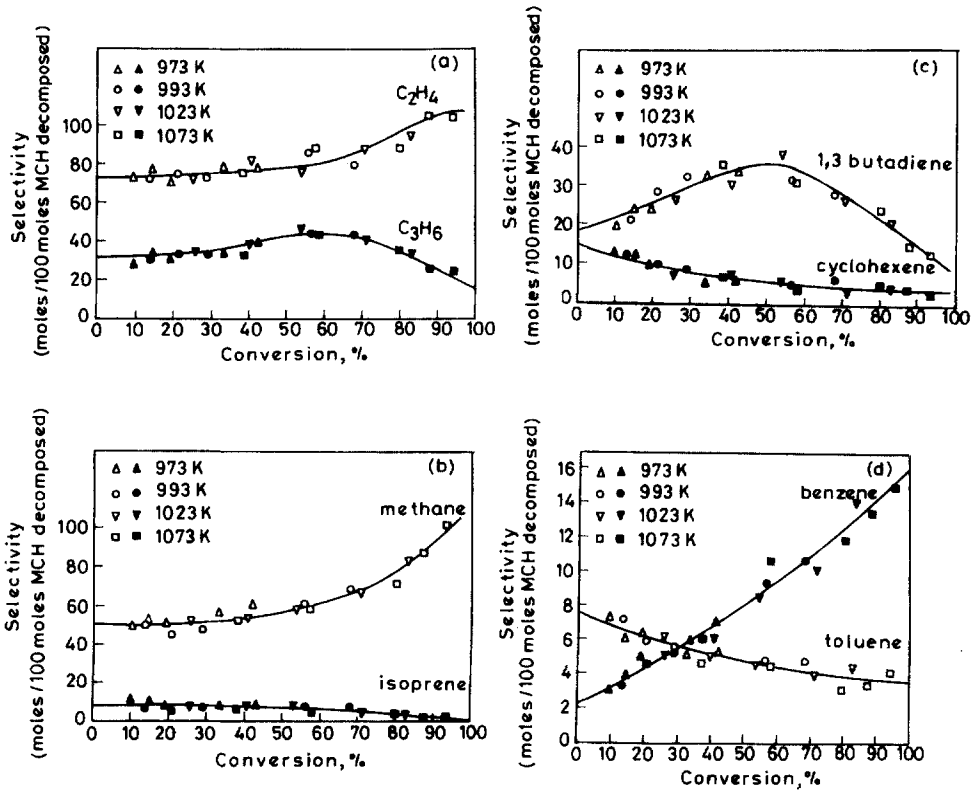

Fig. 4. Variation of product selectivities with conversion.

the kinetic constants of the secondary reactions as well as the initial selectivities of the primary reaction were the same as that used for modeling the thermal pyrolysis data [10]. In the catalytic pyrolysis model, the coke deposition and gasification reactions have not been accounted for. Using this model, the continuity equations for the 14 components (MCH, H_2, CH_4, C_2H_2, C_2H_4, C_2H_6, C_3H_6, C_3H_8, 1,3-C_4H_6, C_4H_8, C_4H_{10}, C_4^+, aromatics and steam) were written for the thermal and catalytic zones. In the catalytic zone, the non-catalysed primary reaction was accounted for in the void space between the catalyst particles and in the pore space within the catalyst, whereas the catalysed primary reaction proceeded on the catalyst surface. It was assumed that, in the catalytic zone, the secondary reactions took place only in the gas phase between the particles and in the pore space.

The continuity equations in each zone were solved using the fourth order Runge–Kutta–Gill algorithm. The numerical integration was based on the actual temperature profile of each run. The simulation model developed was used to compare the experimental and predicted yields at the same conversion. With this basis of comparison, the effect of temperature on individual product selectivities was negligible and, therefore, the experimental and calculated yields obtained at different temperatures have been shown on single plots (Figs. 5–7). As can be seen from these figures, the predicted and the experimental yields of CH_4, C_3H_6, C_4^+ and aromatics were in good agreement for the whole conversion range, whereas the calculated and experimental yields of C_2H_4 and 1,3-C_4H_6 were in good agreement till a conversion of 70%, while at higher conversions, the calculated yields were slightly higher than experimental values.

The axial variation of the calculated conversion and some main products (CH_4, C_2H_4 and C_3H_6) for one run, together with the measured temperature profile and experimental points, is shown in Fig. 8. For this run, the catalyst was placed between 28 and 32 cm from the reactor inlet. As can be seen from the figure, there was a significant increase in conversion in the catalytic zone. Due to the relatively lower temperature in the inlet section, the conversion at the end of the first noncatalytic zone was only 18%. The relative contributions of the catalytic and noncatalytic reactions in the catalytic zone, calculated as $k_c\rho_p(1-\varepsilon_B)/[k_t\varepsilon_B + k_t V_g \rho_p (1-\varepsilon_B)]$, decreased with temperature and varied from 2.7 at 973 K to 0.76 at 1073 K.

5. Coke gasification

The variation of the coke deposited on the catalyst after a run time of 3 h with space time at different temperatures is shown in Fig. 9 and the corresponding plots for the yield of carbon oxides is shown in Fig. 10. Coke is formed due to secondary reactions and increasing the space time or temperature results in an increase in the concentration of coke precursors. At identical conditions, the coke deposited on the unpromoted calcium aluminate was significantly higher whereas the carbon oxide yields were appreciably lower, which confirms that the rate of coke gasification is signifi-

Table 3
Product selectivities in catalytic pyrolysis (moles product/100 moles methylcyclohexane decomposed)

	Run number								
	MA1	MA5	MB1	MB5	MC5	MC6	MC7	MD1	MD5
Temperature, K	973	973	993	993	1023	1023	1023	1073	1073
Feed flow rate g/min	2.40	0.46	2.40	0.46	0.46	0.60	0.40	2.40	0.46
δ, kg steam/ kg MCH	2.5	2.5	2.5	2.5	2.5	2.0	3.0	2.5	2.5
Catalyst weight, g	6.0	3.0	6.0	3.0	3.0	3.0	3.0	6.0	3.0
Conversion %	10.0	42.0	14.0	68.0	82.5	84.0	85.3	38.5	93.5
Methane	49.7	60.5	50.0	68.0	81.6	87.9	87.6	52.0	99.5
Ethane	4.6	6.0	4.9	7.8	8.5	7.0	7.5	3.0	8.5
Ethylene	72.6	76.5	72.8	79.0	94.5	99.6	98.9	74.5	104.
Propane	0.1	0.2	0.1	0.9	0.3	0.3	0.3	0.3	tr
Propylene	28.5	39.0	30.4	44.0	32.8	33.3	32.7	33.0	24.0
Butene-1	0.4	2.2	0.3	1.8	1.1	1.0	1.1	2.2	0.5
1,3-Butadiene	19.8	33.5	21.5	27.5	19.8	20.1	19.3	36.8	12.5
3-Methyl butene-1	1.9	0.4	1.5	0.1	0.2	0.2	0.2	0.4	tr
1,4-Pentadiene	0.6	1.0	1.3	1.8	1.1	1.1	1.0	1.5	0.4
Isoprene	11.8	7.8	9.8	4.0	3.0	2.9	3.1	4.5	0.9
1,*trans*-3-pentadiene	2.0	2.2	1.9	3.1	2.0	1.9	2.0	2.7	1.7
1,*cis*-3-pentadiene	0.9	1.5	0.2	0.6	0.2	0.2	0.2	0.7	tr
Cyclohexene	12.8	5.0	10.8	5.2	3.3	3.2	3.3	5.6	1.8
Benzene	3.0	7.2	3.3	10.7	14.0	14.4	14.3	6.1	15.2
2-Heptene	tr	0.7	0.4	tr	tr	tr	tr	0.6	0.0
Methylcyclopentadiene	0.0	0.5	0.0	0.1	0.4	0.3	0.3	0.3	0.6
Toluene	7.4	5.2	7.3	4.9	4.6	4.5	4.5	4.4	4.2
Cyclohexane	0.0	0.9	1.0	0.7	tr	tr	tr	0.6	0.0
3,Methylcyclohexene + 4,methcyclohexene	3.2	0.4	1.8	0.2	0.2	0.2	0.3	1.6	0.1
1,Methylcyclohexene	4.5	1.6	3.8	0.2	0.2	0.1	0.1	2.0	tr
1,3-Cyclopentadiene	0.0	0.9	0.0	0.4	tr	tr	tr	0.3	tr
1,Methylcyclopentene	0.0	0.5	0.0	0.1	tr	tr	tr	0.5	0.0
1,3-Cyclohexadiene	0.0	0.8	0.0	tr	0.0	tr	tr	tr	0.0
Carbon monoxide	0.1	1.1	0.6	1.6	1.9	1.8	2.5	0.7	1.6
Carbon dioxide	1.5	4.0	1.9	6.2	7.5	4.8	9.9	4.4	10.5
Others	1.0	0.6	0.8	1.2	0.8	0.9	1.1	1.7	1.0
Coke on catalyst after a run time of283 3 h (wt.%)	tr	0.2	0.1	1.5	2.2	2.6	1.2	0.8	3.8
Carbon balance, %	98.6	99.1	95.8	98.5	96.5	97.1	99.1	96.1	95.6

tr = trace.

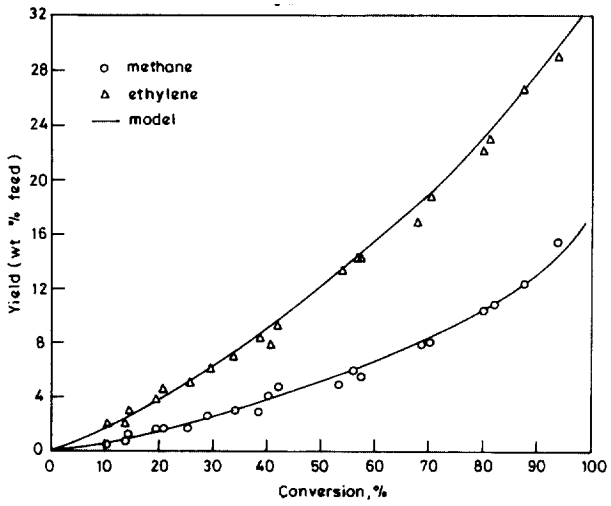

Fig. 5. Comparison between experimental and predicted yields of methane and ethylene.

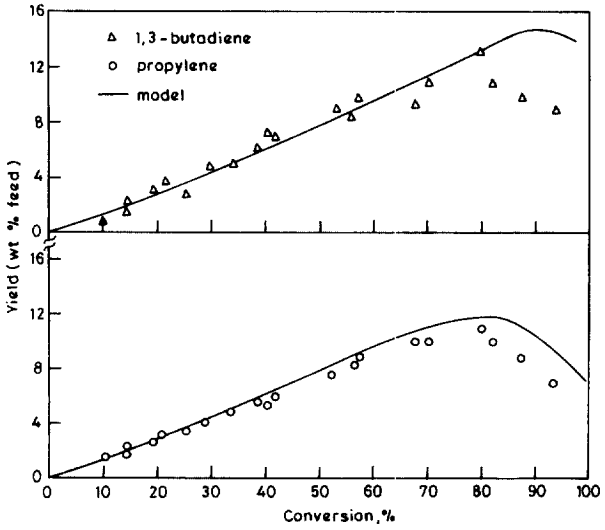

Fig. 6. Comparison between experimental and predicted yields of 1,3-butadiene and propylene.

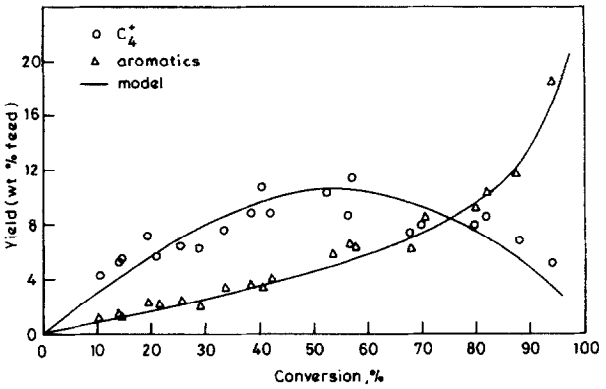

Fig. 7. Comparison between experimental and predicted yields of C_4^+ and aromatics.

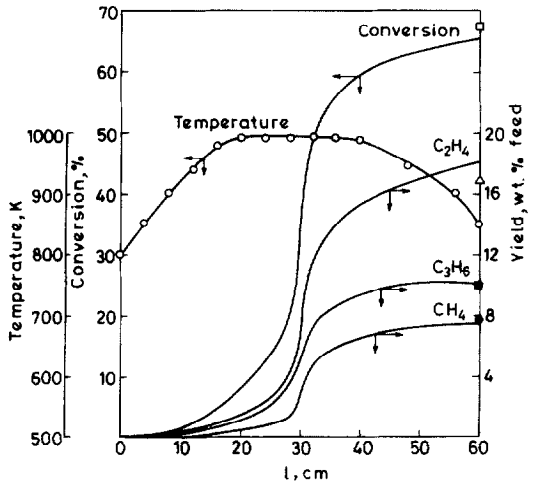

Fig. 8. Axial profiles of calculated conversion and methane, ethylene and propylene yields. (Operating conditions: *n*-heptane flow rate, 0.46 g/min; $\delta = 2.5$ kg steam/kg MCH; catalyst weight, 3.0 g. calculated: (———) experimental: (□), conversion; ●, CH_4; △, C_2H_4; (■), C_3H_6; (○), temperature).

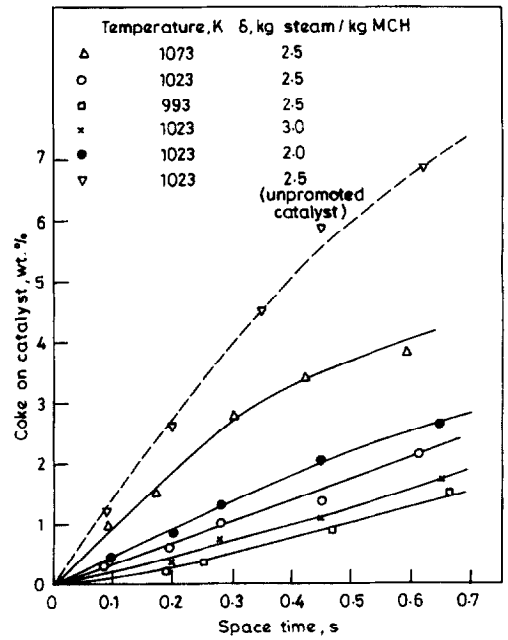

Fig. 9. Effect of space time on coke deposited on catalyst (run time = 3 h).

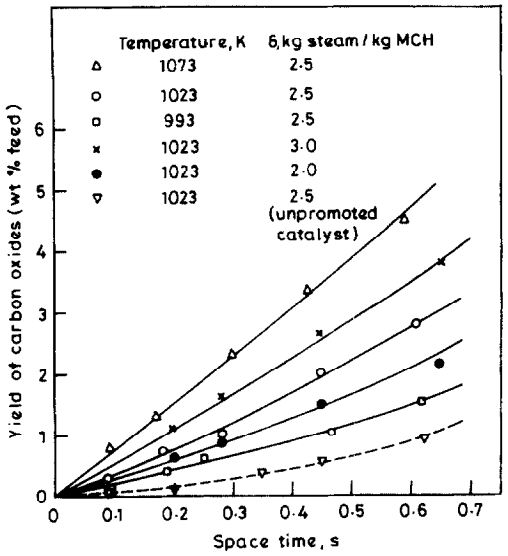

Fig. 10. Effect of space time on carbon oxide yields.

cantly higher on the K_2CO_3 impregnated catalyst. With increasing δ, the coke gasification reaction was enhanced resulting in less coke deposition and higher yield of carbon oxides (Figs. 9 and 10).

To evaluate the kinetics of coke gasification, the rate was expressed as

$$r_g = A_g \exp\left(-\frac{E_g}{RT}\right)(\bar{C}_c)^a p_w^b \qquad (4)$$

r_g was calculated from the rates of coke deposition on the unpromoted and K_2CO_3 impregnated catalysts, and $\bar{C}_c$ was estimated by assuming that the coke deposited on the catalyst varied linearly with run time during a 3 h run. Due to the high steam dilution, the range of variation of p_w was small (0.916–0.944 atm), and, therefore p_w was assumed to be constant for all the runs. Using linear regression, E_g, 'a' and $(A_g\, p_w^b)$ were determined to be 134 kJ/mol, 0.3 and 2.9×10^5 (kg coke/kg cat)$^{0.7}$ h^{-1}, respectively. For the pyrolysis of *n*-heptane on this catalyst, the activation energy for coke gasification was found to be 140 kJ/mol. This value of activation energy is also in good agreement with the value of 154 kJ/mol reported for the K_2CO_3 catalyzed gasification of coke during noncatalytic pyrolysis of *n*-hexane [13].

6. Conclusions

Potassium carbonate impregnated calcium aluminate significantly increases the overall rate of methylcyclohexane pyrolysis but does not have any effect on the hydrocarbon product selectivities. The activation energy for the catalytic pyrolysis is significantly lower than that for noncatalytic pyrolysis. The coke deposited on the catalyst increases with space time and temperature but is lower at higher steam dilution. Incorporation of potassium carbonate to the calcium aluminate catalyst significantly reduces the coke deposition by enhancing the coke-steam reaction. The product yields

obtained can be satisfactorily modeled by a molecular reaction consisting of a first-order primary step and a set of 24 secondary reactions.

7. Nomenclature

a reaction order with respect to coke content of catalyst for coke-steam reaction
A_c cross-sectional area of reactor in the catalytic zone, m^2
A_g preexponential factor for rate constant of coke-steam reaction
b reaction order with respect to steam for coke-steam reaction
$\bar{C}_c$ average coke content of catalyst, kg coke/kg catalyst
E_g activation energy for coke-steam reaction, kJ/mol
k_c catalytic pyrolysis reaction rate constant, $m^3/kg.s$
k_t noncatalytic pyrolysis reaction rate constant, s^{-1}
L_1 reactor length at the end of the first thermal zone, m
L_2 reactor length at the end of the catalytic zone, m
L total reactor length, m
m_{Ao} inlet mass flow rate of methylcyclohexane, kg/s
p_w partial pressure of steam, atm
Q_o inlet volumetric flow rate, m^3/s
r_g rate of catalysed coke-steam reaction (kg coke)/(kg cat) (h)
R gas constant, J/mol K
T reactor temperature, K
V_g void volume of catalyst, m^3/(kg of catalyst)
W mass of catalyst, kg
X_{A1} conversion of methylcyclohexane at the inlet of the catalytic zone
X_{A2} conversion of methylcyclohexane at the end of the catalytic zone

Greek letters

δ mass ratio of steam to methylcyclohexane, kg/kg
ε expansion factor
ε_B void fraction of catalyst bed
ρ_p particle density, kg/m^3
τ space time, s

Acknowledgements

The financial support provided by the Department of Science and Technology, New Delhi, for this study is gratefully acknowledged.

References

[1] T. Tomita, M. Noda, Y. Yamaguchi, K.I. Uwano, British Patent 1,478,899, 1977.
[2] K. Kikuchi, T. Tomita, T. Sakamoto, T. Ishida, Chem. Eng. Prog. 81 (6) (1985) 54.
[3] A.A. Lemonidou, I.A. Vasalos, Appl. Catal. 54 (1989) 119.
[4] S. Nowak, G. Zimmermann, H. Guschel, K. Anders, in: D.L. Trimm (Ed.), Catalysis in Petroleum Refining 1989, Elsevier, Amsterdam, 1990, p. 103.
[5] B. Basu, D. Kunzru, Ind. Eng. Chem. Res. 31 (1992) 146.
[6] R. Mukhopadhyay, D. Kunzru, Ind. Eng. Chem. Res. 32 (1993) 1914.
[7] A.A. Lemonidou, I.A. Vasalos, E.J. Hirschberg, R.J. Bertolacini, Ind. Eng. Chem. Res. 28 (1989) 524.
[8] K.K. Pant, D. Kunzru, Ind. Eng. Chem. Res. 36 (1997) 2059.
[9] V. Anil Kumar, K.K. Pant, D. Kunzru, Appl. Catal. 162 (1997) 193.
[10] K.K. Pant, D. Kunzru, Chem. Eng. J. 67 (1997) 123.
[11] P. Kumar, D. Kunzru, Ind. Eng. Chem. Proc. Des. Dev. 24 (1985) 774.
[12] M. Bajus, V. Vesely, P.A. Leclercq, J.A. Rijks, Ind. Eng. Chem. Prod. Res. Dev. 18 (1979) 135.
[13] T.K. Mandal, D. Kunzru, Ind. Eng. Chem. Proc. Des. Dev. 25 (1986) 794.